




The influence of electrode-tissue-coverage on RF lesion formation and local impedance: Insights from an ex vivo model

Fabian Bahlke MD  | Andreas Wachter MD | Nico Erhard MD | Florian Englert MD | Hannah Krafft MD | Miruna Popa MD | Elena Risse MD | Marc Kottmaier MD | Marta Telishevskaya MD | Sarah Lengauer MD | Carsten Lennerz MD  | Tilko Reents MD | Gabriele Hessling MD | Isabel Deisenhofer MD | Felix Bourier MD 

Department of Electrophysiology, German Heart Center Munich, Technical University of Munich (TUM), Munich, Germany

Correspondence

Fabian Bahlke, MD, Department of Electrophysiology, German Heart Center Munich, Lazarettstr. 36 80636 Munich, Germany.
Email: bahlke@dhm.mhn.de

Abstract

Background: The influence of power, duration and contact force (CF) on radiofrequency (RF) lesion formation is well known, whereas data on local impedance (LI) and electrode-tissue-coverage (ETC) is scarce. The objective was to investigate their effect on lesion formation in an ex vivo model.

Methods and Results: An ex vivo model was developed utilizing cross-sections of porcine heart preparations and a force-sensing, LI-measuring catheter. $N = 72$ lesion were created systematically varying ETC (minor/full), CF (1–5 g, 10–15 g, 20–25 g) and power (20 W, 30 W, 40 W, 50 W). In minor ETC, the distal tip of the catheter was in electric contact with the tissue, in full ETC the whole catheter tip was embedded within the tissue. Lesion size and all parameters were measured once per second ($n = 3320$). LI correlated strongly with lesion depth ($r = -0.742$ for Δ LI; $r = 0.781$ for %LI-drop). Lesions in full ETC were significantly wider and deeper compared to minor ETC ($p < .001$) and steam pops were more likely. Baseline LI, Δ LI, and %LI-drop were significantly higher in full ETC ($p < .001$). In lesions resulting in steam pops, baseline LI, and Δ LI were significantly higher. The influence of CF on lesion size was higher in minor ETC than in full ETC.

Conclusions: ETC is a main determinant of lesion size and occurrence of steam pops. Baseline LI and LI-drop are useful surrogate parameters for real-time assessment of ETC and Δ LI correlates strongly with lesion size.

KEYWORDS

lesion size, local impedance, radiofrequency ablation

ABBREVIATIONS: AI, ablation index; CF, contact force; ETC, electrode-tissue-coverage; FTI, force-time-integral; GI, generator impedance; LI, local impedance; LSI, lesion size index; RF, radiofrequency.

This is an open access article under the terms of the [Creative Commons Attribution-NonCommercial-NoDerivs](https://creativecommons.org/licenses/by-nc-nd/4.0/) License, which permits use and distribution in any medium, provided the original work is properly cited, the use is non-commercial and no modifications or adaptations are made.

© 2023 The Authors. *Pacing and Clinical Electrophysiology* published by Wiley Periodicals LLC.

1 | INTRODUCTION

Sufficient lesion creation using RF-current is a cornerstone for the successful ablation of arrhythmias. Local tissue heating due to high density of current surrounding the catheter tip results in local tissue heating and lesion creation.¹ Several parameters for assessing accurate lesion depth and diameter were evaluated in the past.^{2–5} Impedance changes due to increased ion mobility in heated tissue are known to correlate with lesion dimensions.^{2,6,7} Lesion metric indices can be used as real-time-assessment of lesion size, such as the ablation index (AI, Biosense Webster, Diamond Bar, USA) and lesion size index (LSI, Abbott, Chicago, USA). AI and LSI combine ablation parameters to predict sufficient lesion formation to improve clinical outcomes.^{8–12}

Nevertheless, recovered conduction after the initial, acute conduction block remains a severe issue in RF-ablation, as assessing the actual response of cardiac tissue to ablation remains difficult.¹³ Blood flow, tissue perfusion, and ETC still need to be fully taken into account. Recent data indicate a substantial impact of ETC on lesion size and occurrence of steam pops.¹⁴

Implementing measurements of local impedance (LI), measured between catheter's tip and a proximal electrode in the IntellaNav StablePoint catheter (Boston Scientific, Marlborough, USA), might overcome this deficiency. Generator impedance (GI), measured between the catheter tip and a dispersive electrode, lacks precision due to differences in patients' constitution, blood flow, location of the patches, and patients' gender.^{2,13,15,16} First data on LI and lesion formation was published, but a systematic investigation of the influence of ETC on lesion size and LI is lacking.

This study aimed to investigate the influence of local impedance, ETC, and contact force on lesion geometry using an ex vivo model.

2 | METHODS

2.1 | Ex vivo model

RF-lesions were created using an ex vivo model with porcine cardiac preparations. To allow visualization of lesion formation, cross sections were prepared using ventricular tissue. They were placed inside a saline-filled container with a dispersive electrode within the container. Generator impedance (GI) was kept at 120 Ω by adjusting the ratio of saline and water. Additionally, a heated thermostat (temperature 37°C) and a circulation pump were installed to imitate blood flow. A schematic illustration of the ex vivo setup is shown in Figure 1. The study was approved by the institutional review board.

2.2 | Local impedance and electrode-tissue-coverage

LI values (DirectSense, Boston Scientific, Marlborough, USA) were recorded and measured with an electroanatomic mapping system

(Rhythmia, Boston Scientific, Marlborough, USA) using an open irrigated tip ablation catheter (IntellaNav StablePoint, Boston Scientific, Marlborough, USA).

The catheter uses a local potential field driven by a nonstimulatory alternating current between the distal tip and the forth ring electrode (5 μ A, 14.5 kHz). It subsequently measures the LI between the whole distal tip and the second ring electrode, as previously described.^{17,18}

ETC was defined as the area of electric contact between the RF electrode and adjacent cardiac tissue.¹⁴ In minor ETC, only the distal portion of the RF electrode was in contact with cardiac tissue whereas in full ETC, the whole RF electrode was embedded. Minor and full ETC are represented in Figure 2.

2.3 | Ablation protocol

RF-lesions were created using systematically varied settings of power (20 W, 30 W, 40 W, and 50 W), contact force (1–5, 10–15, and 20–25 g), and electrode-tissue-coverage (minor and full ETC). The catheter was positioned perpendicular to the myocardial tissue. By creating three lesions in every setting of ETC (minor/full), CF (1–5 g, 10–15 g, 20–25 g), and power (20 W, 30 W, 40 W, 50 W), 72 lesions were produced in total. RF was applied for 60 s, unless an audible steam pop occurred. The RF generator (MAESTRO 4000, Boston Scientific) was used in power-controlled mode. According to the clinical settings in the above mentioned catheter, irrigation rate was set to 20 mL/min for ablation with 20 W using 0.9% saline. In ablation with 30 W–50 W, irrigation rate was 30 mL/min.

2.4 | Data collection and measurements

During RF-application all provided ablation data, such as generator and local impedance, temperature, power and RF-time were continuously measured by the Rhythmia system (Boston Scientific, Marlborough, USA). Data was extracted using a screen video of the electroanatomic mapping system (Figure 3).

The complete ex vivo model including the cross sectional preparations and the RF catheter was filmed during 60 s of RF-application with a camera in HD-quality. By this workflow, information regarding lesion size and all ablation parameters were available at any time during 60 s of RF-application. Lesion metrics were measured retrospectively using a digital precision caliper (Meazure, Softonic, Barcelona, Spain). On the basis of change in tissue color, lesion size was defined. Four lesion parameters were measured: diameter at surface, maximum diameter, maximum depth, and depth to maximum diameter. Exemplary measurements of lesion size are shown in Figure 4. A new measurement of all available parameters, including lesion width, depth, LI, GI, CF, temperature, and power was performed, was performed once per second. Thus, multiple measurements per second were done and in total, 3320 data points were collected in 72 lesions. Local and generator impedance drops were calculated as the difference between

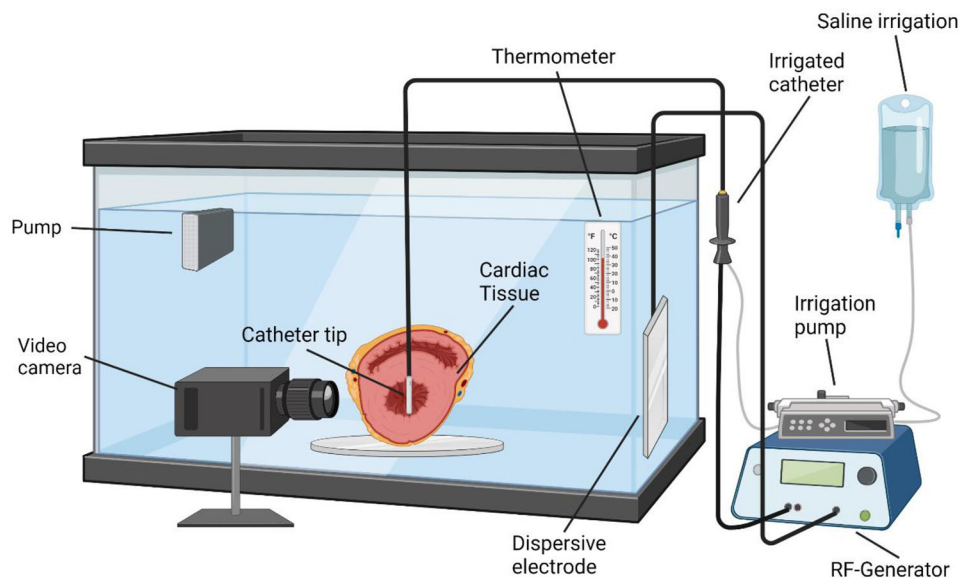


FIGURE 1 Schematic illustration of the experimental setup. The figure was created with BioRender.com. [Color figure can be viewed at wileyonlinelibrary.com]

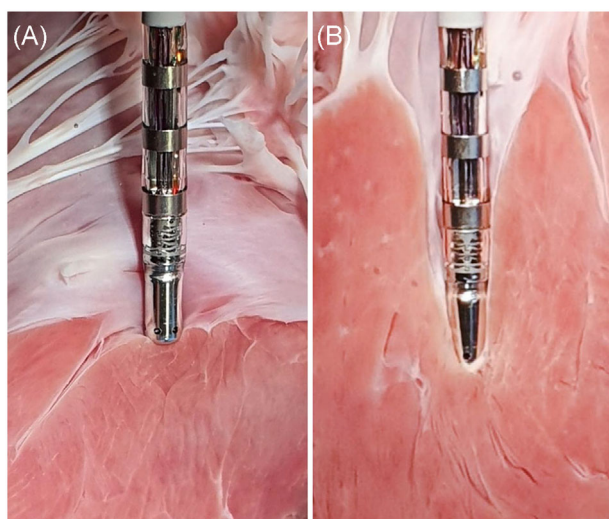


FIGURE 2 Levels of ETC (electrode-tissue-coverage) were defined as minor and full ETC. (A) In minor ETC-level, only the distal end of the catheter is in contact with the tissue. (B) In full ETC-level, the whole catheter tip is in contact with the tissue. ETC, electrode-tissue-coverage. [Color figure can be viewed at wileyonlinelibrary.com]

baseline impedance (measured at the start of RF-application) and current impedance.

2.5 | Statistical analysis

Statistical analysis was performed by using the SPSS Statistics v28.0 software. Continuous variables are described as mean \pm standard deviation. Statistical significance was estimated with the Student's *t*-

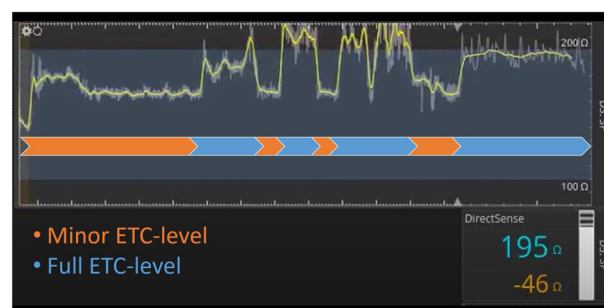


FIGURE 3 Timeline of LI in vivo in different ETC-levels. Illustrated in orange, the catheter position was in minor ETC-level. Catheter was moved into a pouch of cardiac tissue to accomplish full ETC-level (illustrated in blue). ETC, electrode-tissue-coverage; LI, local impedance. [Color figure can be viewed at wileyonlinelibrary.com]

test or the Mann-Whitney-*U*-test if normal distribution was rejected. Categorical variables were analyzed with the chi-square or Fisher's exact test and compared with odds-ratios. All significance tests were two-tailed with rejecting the null hypothesis at $p < .05$.

3 | RESULTS

In total, 3320 measurements of lesion depth and diameter, LI, GI, CF, and temperature were calculated. Twenty steam pops occurred. In all lesions ($n = 72$), mean diameter at the end of RF application was 9.51 ± 1.91 mm, mean depth 7.29 ± 2.50 mm. Baseline LI was higher compared to baseline GI ($268.78 \pm 50.19 \Omega$ and $150.97 \pm 22.51 \Omega$).

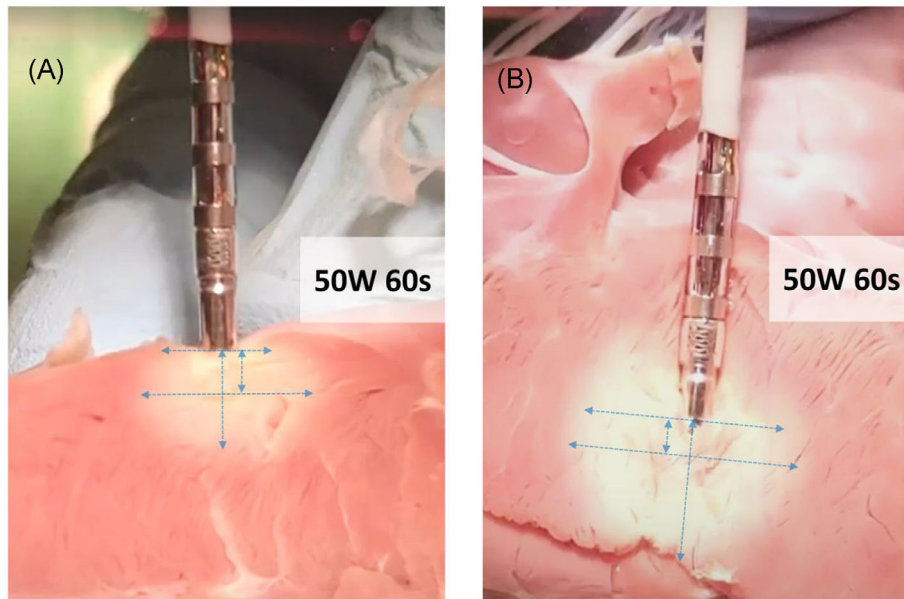


FIGURE 4 Exemplary measurements of lesion size in minor ETC (A) and full ETC (B). Measurements included surface diameter, maximum diameter, maximum depth and depth of maximum diameter. [Color figure can be viewed at wileyonlinelibrary.com]

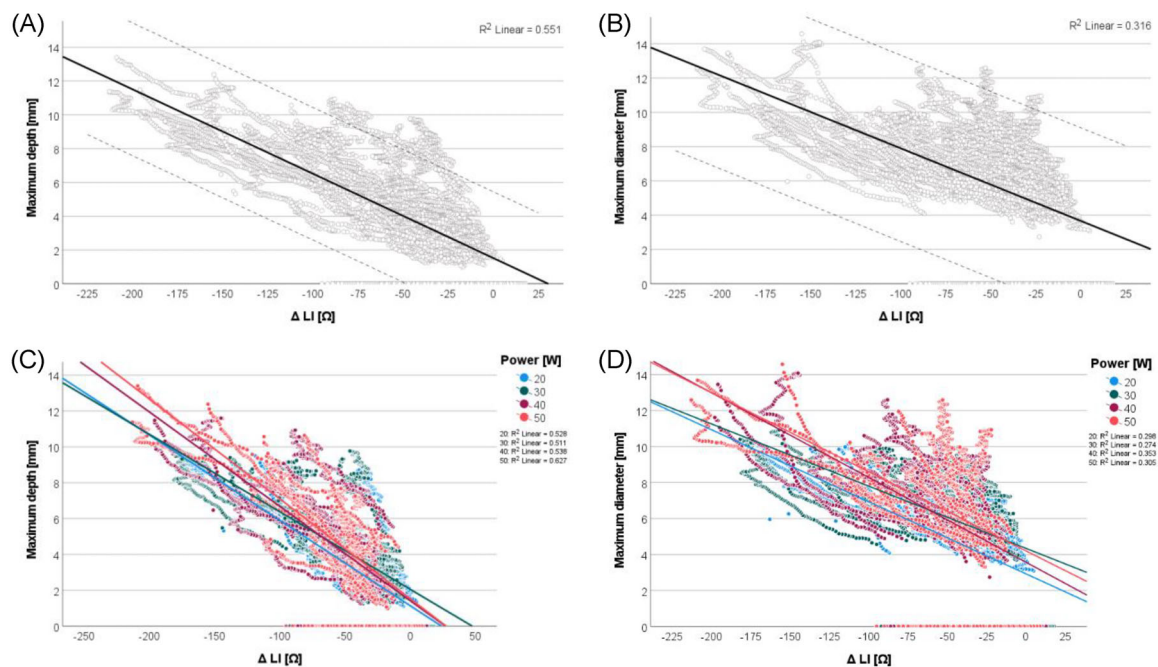


FIGURE 5 Scatter plots of Δ LI and lesion depth (A) and diameter (B). Scatter plots of Δ LI and lesion depth (C) and diameter (D) in all power levels from 20 to 50 W. LI, local impedance. [Color figure can be viewed at wileyonlinelibrary.com]

3.1 | Correlation of local impedance and lesion size

Significant correlations were observed between LI changes and lesion geometrics, including all measurements. Lesion depth and diameter correlate strongly with Δ LI ($r = -0.742$ for depth and $r = -0.562$ for

diameter, $p < .001$) and %LI drop ($r = 0.781$ for depth and $r = 0.655$ for diameter, $p < .001$). Δ LI also correlated strongly with final lesion depth and diameter ($r = -0.75$ and $r = -0.58$, $p < .001$). Figure 5A,B show scatter plots of measured lesion metrics and LI drop. Figure 5C,D differentiate correlations in selected power level from 20 to 50 W.

TABLE 1 Lesion characteristics in minor and full ETC-level.

	Minor ETC (n = 36)	Full ETC (n = 36)	p-value
Diameter surface [mm]	7.41 ± 1.14	8.68 ± 1.28	<.001
Diameter intramural [mm]	8.48 ± 1.61	10.54 ± 1.63	<.001
Maximum depth [mm]	5.13 ± 0.99	9.45 ± 1.45	<.001
Start LI [Ω]	236.89 ± 26.42	300.67 ± 21.61	<.001
Start GI [Ω]	150.61 ± 21.61	151.33 ± 23.68	.893
Δ LI [Ω]	-53.61 ± 24.84	-125.53 ± 46.04	<.001
Δ GI [Ω]	-21.33 ± 10.81	-33.44 ± 11.80	<.001
%LI drop [%]	22.14 ± 8.62	40.63 ± 10.07	<.001
%GI drop [%]	13.85 ± 6.08	22.56 ± 8.12	<.001
Duration of RF-application [s]	54.00 ± 13.07	47.11 ± 17.57	.032
Mean progression in diameter per second [mm/s]	0.17 ± 0.08	0.28 ± 0.19	<.001
Mean progression in depth per second [mm/s]	0.11 ± 0.05	0.26 ± 0.18	<.001

Abbreviations: ETC, electrode-tissue-coverage; GI, generator impedance; LI, local impedance.

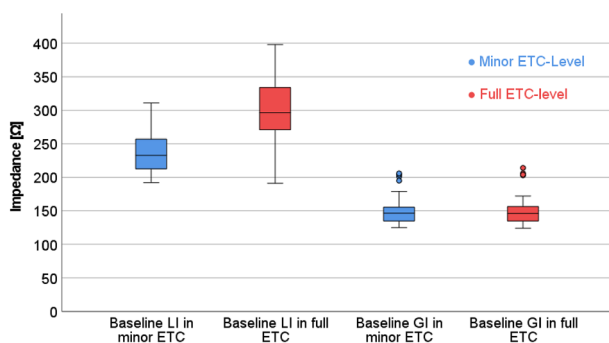


FIGURE 6 Lesion size in different ETC-levels. (A) Final lesion depth. (B) Final lesion diameter. ETC, electrode-tissue-coverage. [Color figure can be viewed at wileyonlinelibrary.com]

3.2 | Influence of ETC-level on lesion metrics

As shown in Table 1 and Figure 6, all lesion metrics and LI changes differ significantly in ETC-levels ($p < .001$). Lesions are wider and deeper in full ETC-level compared to minor ETC-levels (Table 1). Beyond that, average growth (measured in mm/s) was significantly higher in full ETC (Table 1). These findings are observed at all power levels (Tables 2 and 3). Due to differences in occurrence and timing of steam pops, RF-duration differs significantly in ETC-levels ($54.00 \text{ s} \pm 13.07 \text{ s}$ and $47.11 \text{ s} \pm 17.57 \text{ s}$; $p = .032$).

Differences were also seen in baseline impedance: Baseline LI was significantly higher in full ETC-level, but GI did not differ (Table 1 and Figure 7).

3.3 | Influence of contact force on lesion metrics

Mean CF in lesions with 1–5 g was $4.08 \pm 1.65 \text{ g}$, in lesions with aimed CF of 10–15 g mean CF was $12.09 \pm 2.49 \text{ g}$. Mean CF in lesions with 20–

25 g was $21.89 \pm 3.99 \text{ g}$. Correlations between CF-level and final lesion size were weak $r = 0.262$ ($p = .026$) for lesion diameter and 0.143 for lesion depth ($p = .230$).

Analyzing ETC-levels separately, final lesion size and CF-level correlated stronger in minor ETC-level ($r = 0.531$; $p < .001$ for lesion diameter and 0.409; $p = .013$ for lesion depth) than in full ETC-level ($r = 0.160$; $p = .35$ for lesion diameter and $r = 0.183$; $p = .284$ for lesion depth).

Including all lesions in all ETC-levels into analysis, no significant differences in lesion size were observed except for lesion diameter in CF-level 1 and 3 ($8.89 \pm 2.18 \text{ mm}$ and $10.06 \pm 1.68 \text{ mm}$, $p = .042$). Figure 8 illustrates this finding below.

Analyzing lesions in minor ETC-level only, the impact of CF on lesion metrics becomes more relevant. Lesions became wider and deeper using 20–25 g of CF compared to lesions created with 1–5 g (s. Table 4). Significant differences in lesion metrics comparing CF-level 1 and 2 were observed in maximum lesion diameter ($7.34 \pm 1.49 \text{ mm}$ and $8.62 \pm 1.17 \text{ mm}$, $p = .014$), but not in lesion depth ($4.67 \pm 1.10 \text{ mm}$ and $5.11 \pm 0.65 \text{ mm}$, $p = .12$). Comparing CF-level 2 and 3, the only parameter varying significantly was surface diameter ($7.63 \pm 0.70 \text{ mm}$ and $8.26 \pm 0.70 \text{ mm}$, $p = .019$).

3.4 | Characteristics of lesions with steam pops

In lesions with occurrence of a steam pop, baseline LI was significantly higher (Figure 9, Table 5). Despite shorter RF-duration due to stopping of energy delivery after occurrence of a steam pop, lesions did not differ in diameter and depth. The velocity of lesion growth was significantly higher in lesions with steam pops. Lesion metrics, changes in LI and GI and further information about lesions with steam pops is illustrated in Table 5. In Tables 6 and 7, characteristics are differentiated between all power levels from 20–50 W. Timing of steam pops is illustrated in Figure 10 as a Kaplan–Meier-analysis.

TABLE 2 Lesion characteristics and impedance changes in lesions at 20 and 30 W differentiated between ETC-levels.

	20 W			30 W		
	Minor ETC (n = 9)	Full ETC (n = 9)	p-value	Minor ETC (n = 9)	Full ETC (n = 9)	p-value
Diameter surface [mm]	6.53 ± 0.77	8.11 ± 0.41	<.001	7.45 ± 1.30	8.54 ± 0.82	.050
Diameter intramural [mm]	7.01 ± 0.76	9.82 ± 0.33	<.001	8.30 ± 1.43	10.19 ± 0.45	.002
Maximum depth [mm]	4.29 ± 0.44	8.97 ± 0.34	<.001	5.08 ± 0.80	9.33 ± 0.30	<.001
Start LI [Ω]	247.44 ± 25.15	316.67 ± 47.92	.001	230.33 ± 27.21	288.44 ± 51.27	.008
Start GI [Ω]	153.44 ± 13.81	159.22 ± 20.21	.245	154.67 ± 25.79	158.44 ± 30.75	.781
Δ LI [Ω]	-41.89 ± 18.90	-128.78 ± 45.39	<.001	-52.44 ± 24.89	-117.22 ± 50.26	.003
Δ GI [Ω]	-16.56 ± 6.98	-36.00 ± 13.54	.001	-20.78 ± 10.23	-33.56 ± 14.00	.042
%LI drop [%]	16.51 ± 6.31	39.70 ± 10.27	<.001	22.11 ± 8.26	39.02 ± 11.58	.003
%GI drop [%]	10.58 ± 3.81	22.95 ± 8.48	.001	13.24 ± 6.18	22.11 ± 9.92	.037
Duration of RF-application [s]	60.00 ± 0.00	60.00 ± 0.00	-	60.00 ± 0.00	57.78 ± 6.67	0.33
Mean progression in diameter per second [mm/s]	0.12 ± 0.01	0.17 ± 0.01	<.001	0.14 ± 0.02	0.18 ± .02	.002
Mean progression in depth per second [mm/s]	0.07 ± 0.01	0.15 ± 0.01	<.001	0.09 ± 0.01	0.16 ± 0.02	<.001

Abbreviations: GI, generator impedance; LI, local impedance.

TABLE 3 Lesion characteristics and impedance changes in lesions at 40 and 50 W differentiated between ETC-levels.

	40 W			50 W		
	Minor ETC (n = 9)	Full ETC (n = 9)	p-value	Minor ETC (n = 9)	Full ETC (n = 9)	p-value
Diameter surface [mm]	7.89 ± 1.11	9.32 ± 1.67	.048	7.79 ± 0.85	9.48 ± 1.48	.009
Diameter intramural [mm]	9.12 ± 1.02	11.01 ± 2.32	.040	9.52 ± 1.82	11.22 ± 2.11	.043
Maximum depth [mm]	5.60 ± 0.74	9.55 ± 1.96	<.001	5.57 ± 1.28	10.07 ± 2.12	<.001
Start LI [Ω]	232.67 ± 19.57	292.33 ± 42.26	.001	237.11 ± 33.24	305.22 ± 53.68	.005
Start GI [Ω]	149.22 ± 22.98	147.89 ± 24.58	.907	145.11 ± 24.42	139.78 ± 14.27	.581
Δ LI [Ω]	-62.44 ± 30.12	-127.44 ± 44.00	.002	-57.67 ± 23.54	-128.67 ± 51.42	.002
Δ GI [Ω]	-26.22 ± 14.02	-32.33 ± 10.57	.312	-21.78 ± 10.39	-31.89 ± 10.33	.055
%LI drop [%]	26.23 ± 10.70	42.69 ± 9.13	.003	23.73 ± 6.87	41.10 ± 10.57	<.001
%GI drop [%]	17.01 ± 7.70	22.36 ± 8.04	.168	14.59 ± 5.01	22.83 ± 7.28	.013
Duration of RF-application [s]	57.22 ± 8.33	40.11 ± 19.85	.030	40.00 ± 19.29	31.89 ± 17.63	.366
Mean progression in diameter per second [mm/s]	0.17 ± 0.04	0.32 ± 0.12	.002	0.27 ± 0.09	0.46 ± 0.28	.040
Mean progression in depth per second [mm/s]	0.10 ± 0.03	0.28 ± 0.10	<.001	0.16 ± 0.05	0.43 ± 0.27	.011

Abbreviations: GI, generator impedance; LI, local impedance

4 | DISCUSSION

The present study analyzed the interplay of electrode-tissue-coverage, lesion size, local impedance, and occurrence of steam pops. There are four main findings, which are described below:

(1) ETC is a primary determinant of lesion formation

Among analyzed parameters, ETC-level has shown to be a main determinant for lesion size. In full ETC-level, lesions were wider

(1.24 fold) and deeper (1.84 fold), while lesion growth occurred at higher velocity (mean progression in lesion depth per second 0.11 ± 0.05 mm/s vs. 0.26 ± 0.18 mm/s; $p < .001$). 30 W lesions in full ETC-level were deeper compared to lesions with 50 W and minor ETC (Figure 6).

Yet, in our experimental setup, energy delivery was stopped in case of a steam pop. This should be considered, as lesions became significantly wider and deeper in full ETC-level despite the more frequent occurrence of steam pops and consequently the shorter time of potential lesion formation. This aspect is also seen in a significantly

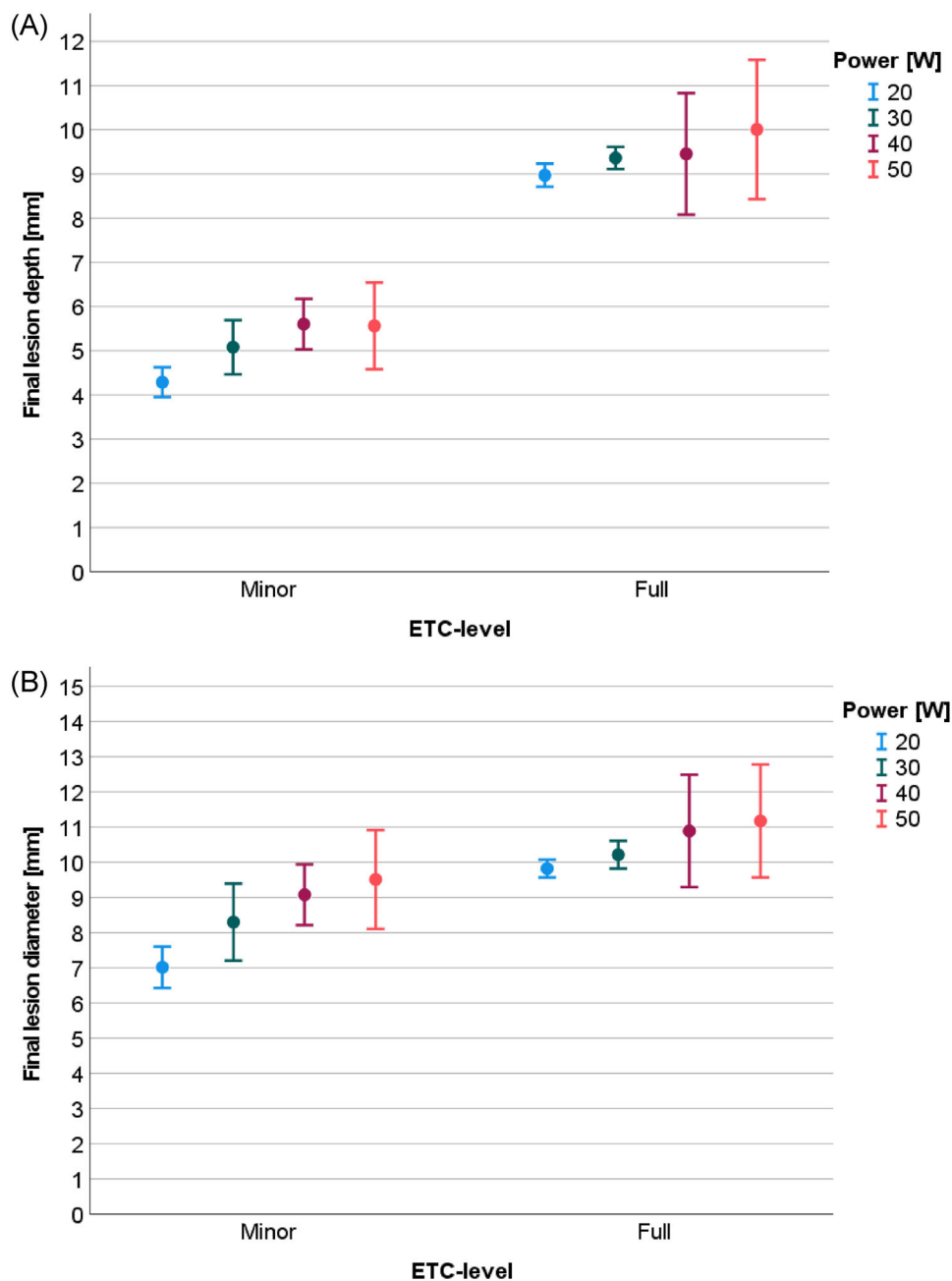


FIGURE 7 Boxplot of local impedance and generator impedance at baseline in minor (blue) and full (red) ETC-level. ETC, electrode-tissue-coverage; GI, generator impedance; LI, local impedance. [Color figure can be viewed at wileyonlinelibrary.com]

higher velocity of lesion growth in full ETC, as shorter RF duration is considered in this parameter (Table 1).

Additionally, baseline LI (240.2 Ω vs. 297.8 Ω , $p < .001$), Δ GI, Δ LI, %LI drop, and %GI drop were significantly higher in full ETC. Baseline GI did not differ between both ETC-levels (s. Table 1).

In a clinical scenario, increasing power seems to have a minor impact on lesion growth compared to different ETC-levels. Consequently, expected ETC should be considered in clinical practice. Trabeculation in the atria or ventricles may lead to larger lesions. On the contrary, ablation at even areas, such as the posterior wall of the left atrium, may result in smaller lesions. Still, predicting the actual ETC-level in

vivo remains a problem. Evaluating baseline impedance and impedance changes might be an approach for this issue.

In clinical practice, the LI curve progression may indicate changes in ETC. Between blood pool and first endocardial contact, an initial rise in LI graph curve can be seen. When further advancing the tip into trabeculated areas of the endocardium, there will be additional rise in the impedance graph, enabling the operator to estimate changes in ETC.

Interestingly, baseline GI did not differ in different ETC-levels, while baseline LI did (see Figure 7). Additionally, LI drops in full ETC were significantly higher compared to minor ETC-levels (s. Table 1).

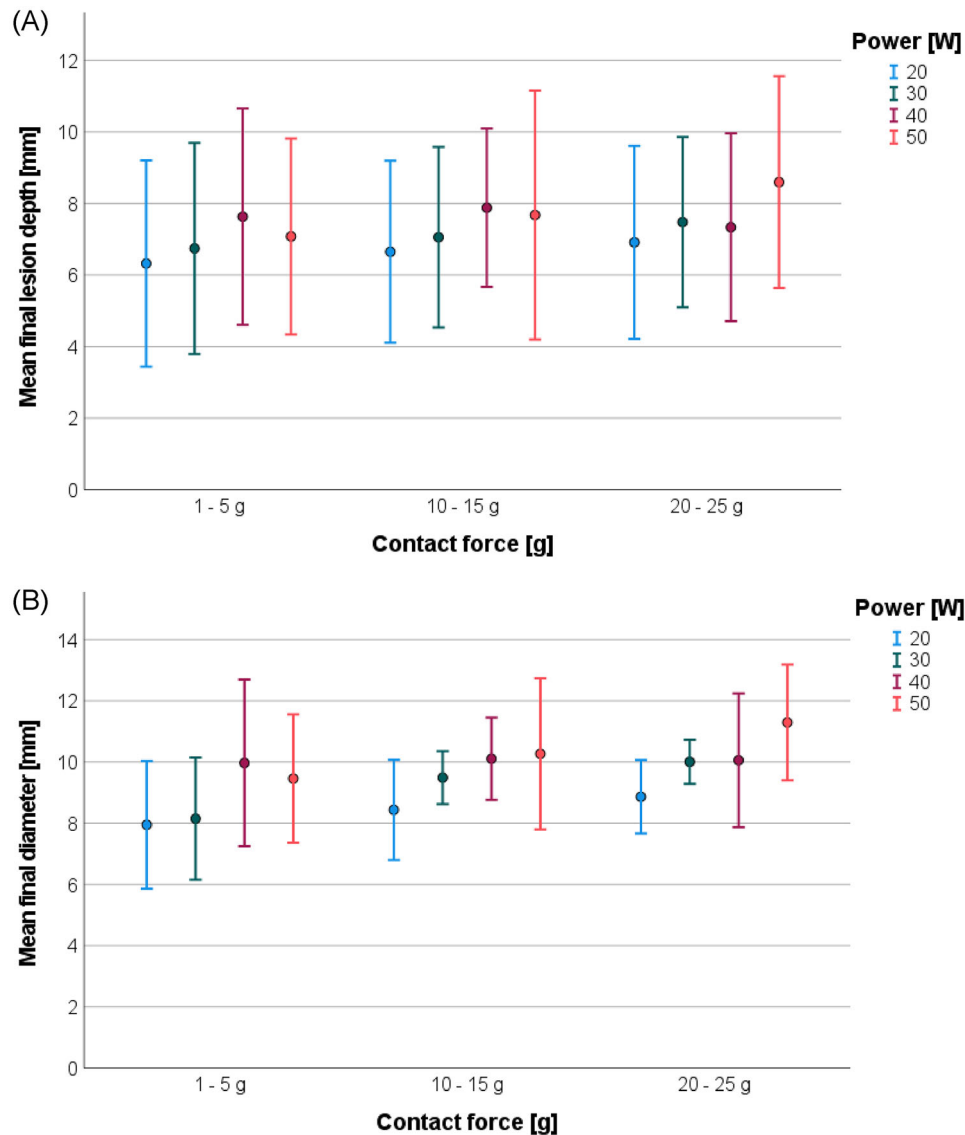


FIGURE 8 Final lesion depth (A) and diameter (B) after complete RF-application. Values were split into all CF-levels (1–5 g, 10–15 g, 20–25 g) and power levels (20–50 W). Error bars indicate 95%-CI. CF, contact force. [Color figure can be viewed at wileyonlinelibrary.com]

The catheter's technique of LI measurement can impact values of LI. As the proximal and distal ring electrode are part of LI calculation, the proximity of these electrodes to cardiac tissue affects baseline LI. We assume that greater proximity of the distal ring electrode to cardiac tissue results in higher values of LI aiding in the differentiation of ETC levels in clinical practice.

In a synopsis of these findings, baseline LI and the extent of LI drop should be monitored during the RF application to predict ETC-levels and, consequently lesion size.

(2) Strong correlation of LI drop and lesion size

In accordance with previous publications,^{19,20} %LI drop correlated strongest with lesion size, especially with lesion depth ($r = 0.781$) while a weaker correlation was seen with lesion diameter ($r = 0.655$). We added valuable information on the temporal evolution of LI and

lesion formation, as we were able to monitor changes in LI throughout the whole RF application of 60 s. Furthermore, a strong correlation can be considered in all power settings (20–50 Watt, s. Figure 5).

Thus, LI drop can be used as a real-time surrogate parameter for sufficient lesion formation, even in high power ablation.

(3) Characteristics of lesions with steam pops and impact of LI on safety

No significant differences in lesion metrics of RF-applications with and without steam pops were observed. An explanation for this might be a shorter RF-duration in lesions with steam pops ($60.00 \text{ s} \pm 0.00 \text{ s}$ and $27.15 \text{ s} \pm 11.08 \text{ s}$; $p < .001$). Baseline LI, LI-drop, and %LI-drop were significantly higher in lesions with steam pops. A greater ETC-level is associated with higher risks of steam pops.¹⁴ The underlying mechanism for this finding seems to be less current dissipating into saline.

TABLE 4 Differences in ablation parameters and lesion metrics at the end of RF-application. Only lesions created with minor ETC-level were included in analysis.

	CF-level 1 (1–5 g)	CF-level 3 (20–25 g)	p-value
Diameter surface [mm]	6.35 ± 1.03	8.26 ± 0.70	<.001
Maximum diameter [mm]	7.34 ± 1.49	9.47 ± 1.45	.002
Maximum depth [mm]	4.67 ± 1.10	5.61 ± 1.00	.038
Start LI [Ω]	228.25 ± 22.27	244.08 ± 21.64	.091
Start GI [Ω]	144.08 ± 12.01	155.50 ± 23.53	.15
Δ LI [Ω]	−43.00 ± 16.23	−62.00 ± 20.28	.019
Δ GI [Ω]	−17.25 ± 7.54	−23.50 ± 9.53	.089
%LI drop [%]	18.58 ± 7.37	25.30 ± 7.38	.022
%GI drop [%]	11.81 ± 4.49	15.04 ± 5.92	.146

Abbreviations: CF, contact force; GI, generator impedance; LI, local impedance.

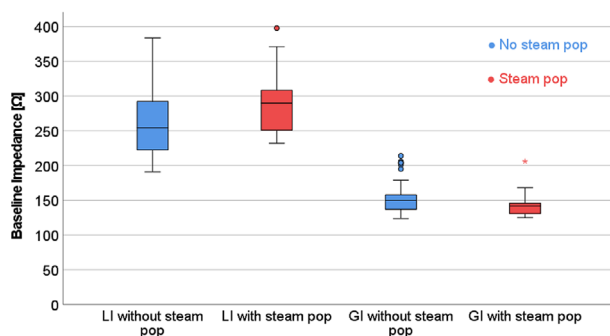


FIGURE 9 Boxplot of baseline LI and GI in lesions with (red) and without (blue) steam pops. GI, generator impedance; LI, local impedance. [Color figure can be viewed at wileyonlinelibrary.com]

As mentioned above, baseline LI and LI-drop remain suitable parameters for real-time assessment of the ETC-level and lesion metrics. Therefore, evaluating both might help create durable lesions, predict the ETC-level, as well as increase safety of catheter ablation. For instance, in case of a high baseline LI and high LI-drops at the beginning of a RF-application, stopping current delivery should be considered.

(4) Influence of ETC and CF on lesion size

CF-level did not correlate strongly with resulting lesion size when all ETC-levels were included in the analysis. One possible explanation for this might be that although CF provides valuable information about the mechanical pressure on the catheter tip (mainly axial), less information about the actual coverage between the electrode and tissue is gathered. However, the latter seems to be most decisive for the amount of current dissipating into the saline in our experimental setup or into the blood pool in clinical settings. The following two aspects support this assumption.

- While lesion metrics did not vary in different CF-levels, including all lesions in analysis, a subgroup analysis showed significant differences. In minor ETC-level, CF exceeding 10 g was decisive for larger lesions. Correlations between CF-level and final lesion size also improved clearly. Remarkably, the influence of higher CF declines more rapidly regarding lesion depth, while sufficient CF seems to be more decisive for lesion width. This might be due to a higher ETC at the edges of the catheter tip.
- While steam pops occurred in all CF-levels, one took place in a setting using 30 W after 40 s. In this RF-application CF did not exceed 6 g of contact force (mean CF 5 g) when performed with full ETC.

Thus, it can be stated that ETC mainly influences lesion metrics and the occurrence of steam pops. However, CF remains an important factor for lesion formation, but seems to be of secondary importance, when ETC-level rises. On the other hand, creating durable lesions is possible even with little CF, if higher ETC-levels are achieved.

CF for itself provides important feedback in terms of safety for the operator but lacks physiological feedback on tissue characteristics and tissue response.¹³ Kumar et al. suggest this might be due to a weak correlation of CF and baseline GI.²¹

This finding was also reproduced in our data regarding the correlation of CF and baseline GI. Previous data from Matsuura et al. and Tsutsui et al. revealed rising values of baseline LI when CF was increased.^{17,22} The influence of a higher CF on baseline LI was lower when the catheter was positioned in 90° compared to 30° and 45°.¹⁷

In our study, we also observed a statistical trend towards a rising baseline LI in CF-level 3 compared to CF-level 1 (228.25 ± 22.27 Ω vs. 244.08 ± 21.64 Ω; $p = 0.091$), as illustrated in Table 4. However, this trend was only observed in minor ETC. We assume that the reason for this finding is mainly a higher ETC, which is accomplished due to the mechanical pressure on the catheter's tip. It seems reasonable, that CF does not increase baseline LI in full ETC, as the maximum coverage is already achieved and cannot be increased by rising values of CF.

Despite little impact of CF on lesion size and values of LI in full ETC, monitoring CF in the clinical routine remains essential.²³

The possibility of combining CF with other parameters into the force-time-integral or ablation indices improves predictive values for lesion formation.^{8–10,24}

However, besides these benefits of CF and further combinations into FTI, AI, or LSI, the ability to assess the actual tissue response is lacking.

5 | LIMITATIONS

First, ex vivo experiments cannot be fully transferred to the clinical setting in vivo. All lesions were created under idealized conditions. Measured values of GI and LI might be systematically elevated, as missing tissue perfusion in an ex vivo model has to be considered. One consequence is that the current density around the catheter might rise as less current dissipates. This elevates the risk for steam pops and

TABLE 5 Lesion characteristics and impedance changes in lesions with steam pops compared to lesion without steam pops.

	No steam pop (n = 52)	Steam pop (n = 20)	p-value
Diameter surface [mm]	8.01 ± 1.38	8.44 ± 1.46	.254
Diameter intramural [mm]	9.40 ± 1.86	9.80 ± 2.06	.420
Maximum depth [mm]	6.98 ± 2.36	8.12 ± 2.71	.082
Start LI [Ω]	260.81 ± 50.20	289.50 ± 44.97	.024
Start GI [Ω]	153.96 ± 23.38	143.20 ± 18.41	.069
Δ LI [Ω]	-80.21 ± 50.73	-113.75 ± 46.82	.011
Δ GI [Ω]	-25.73 ± 13.47	-31.70 ± 9.83	.076
%LI drop [%]	28.77 ± 13.23	38.19 ± 10.48	.003
%GI drop [%]	16.68 ± 8.53	22.17 ± 6.55	.012
Duration of RF-application [s]	60.00 ± 0.00	27.15 ± 11.08	<.001
Mean progression in diameter per second [mm/s]	0.16 ± 0.03	0.41 ± 0.19	<.001
Mean progression in depth per second [mm/s]	0.12 ± 0.04	0.34 ± 0.20	<.001

Abbreviations: GI, generator impedance; LI, local impedance.

TABLE 6 Lesion characteristics and impedance changes in lesions with and without steam pops differentiated between 20 and 30 W.

	20 W			30 W		
	Steam pop (n = 0)	No steam pop (n = 18)	p-value	Steam pop (n = 1)	No steam pop (n = 17)	p-value
Diameter surface [mm]	-	7.32 ± 1.01	-	7.95	8.00 ± 1.23	.968
Diameter intramural [mm]	-	8.42 ± 1.55	-	9.39	9.23 ± 1.46	.919
Maximum depth [mm]	-	6.63 ± 2.44	-	8.76	7.11 ± 2.30	.496
Start LI [Ω]	-	282.06 ± 51.45	-	296.00	257.24 ± 50.45	.466
Start GI [Ω]	-	156.33 ± 17.05	-	145.00	157.24 ± 28.29	.680
Δ LI [Ω]	-	-85.33 ± 56.00	-	-121.00	-82.71 ± 51.64	.481
Δ GI [Ω]	-	-26.28 ± 14.47	-	-41.00	-26.35 ± 13.55	.309
%LI drop [%]	-	28.18 ± 14.46	-	40.88	29.96 ± 13.21	.433
%GI drop [%]	-	16.76 ± 9.01	-	28.28	17.05 ± 9.11	.249
Duration of RF-application [s]	-	60.00 ± 0.00	-	40.00	60.00 ± 0.00	-
Mean progression in diameter per second [mm/s]	-	0.14 ± 0.03	-	.23	0.15 ± 0.02	.008
Mean progression in depth per second [mm/s]	-	0.11 ± 0.04	-	.22	0.12 ± 0.04	.022

Abbreviations: GI, generator impedance; LI, local impedance.

might be an explanation for frequent steam pops in this study. However, recently published data compared an ex vivo setup comparable to our model with an in vivo model and observed a strong reproducibility in both models.²⁵

Second, the maximum power in this study was 50 W. In the clinical use of high power short duration (HPSD) ablation, power settings up to 90 W are possible. Consequently, our findings cannot be transferred to very HPSD-settings without prior verification. However, the only catheters that can measure LI are the IntellaNav MIFI and StablePoint (both Boston Scientific, Marlborough, USA), with the highest authorized power of 50 Watts at the time of publication.

Third, irrigation was set to clinical recommendations of the manufacturer (20 mL/min in 20 W, 30 mL/min in 30–50 W). Therefore, we avoided comparing lesion formation at 20 W and other power levels.

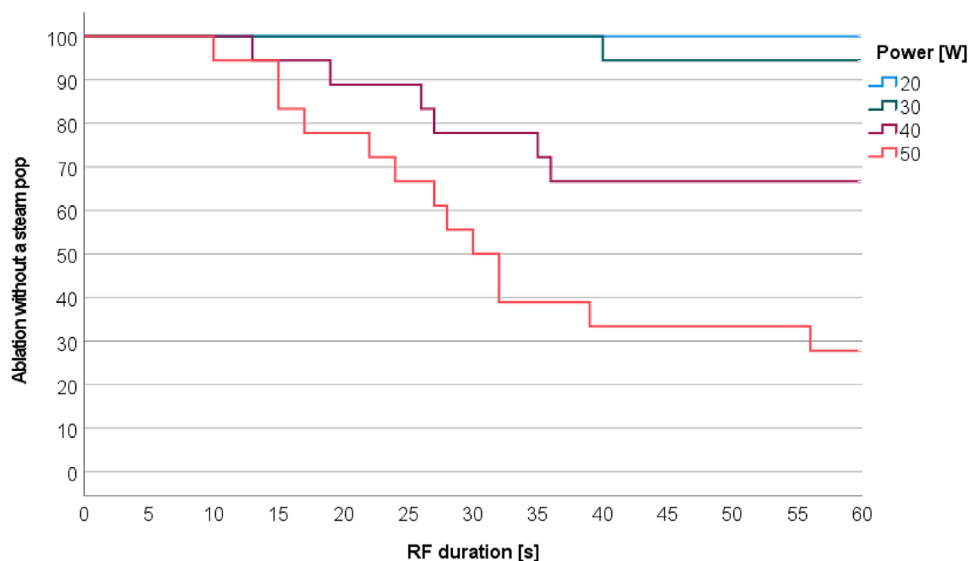
6 | CONCLUSION

ETC-level is a main determinant for lesion size and occurrence of steam pops. Baseline LI and the extent of LI drop might be good surrogates for real-time assessment of ETC-level.

TABLE 7 Lesion characteristics and impedance changes in lesions with and without steam pops differentiated between 40 and 50 W.

	40 W			50 W		
	Steam pop (n = 6)	No steam pop (n = 12)	p-value	Steam pop (n = 13)	No steam pop (n = 5)	p-value
Diameter surface [mm]	8.19 ± 1.04	8.82 ± 1.76	.434	8.63 ± 1.70	8.66 ± 0.59	.973
Diameter intramural [mm]	9.39 ± 1.56	10.40 ± 2.16	.323	10.09 ± 2.37	11.12 ± 0.97	.366
Maximum depth [mm]	7.93 ± 1.74	7.40 ± 2.84	.679	8.23 ± 3.25	6.73 ± 1.13	.336
Start LI [Ω]	278.33 ± 43.48	254.58 ± 44.37	.297	294.15 ± 48.22	211.40 ± 5.86	.002
Start GI [Ω]	136.33 ± 7.34	154.67 ± 26.03	.115	146.23 ± 21.91	132.60 ± 4.83	.195
Δ LI [Ω]	-118.33 ± 42.83	-83.25 ± 50.15	.163	-111.08 ± 51.81	-46.60 ± 16.24	.016
Δ GI [Ω]	-33.83 ± 7.39	-27.00 ± 14.06	.286	-30.00 ± 10.84	-18.60 ± 8.62	.052
%LI drop [%]	41.54 ± 8.04	30.92 ± 13.58	.099	36.44 ± 11.73	21.95 ± 7.45	.022
%GI drop [%]	24.66 ± 4.21	17.20 ± 8.58	.064	20.55 ± 7.18	13.91 ± 6.19	.088
Duration of RF-application [s]	26.00 ± 8.94	60.00 ± 0.00	<.001	26.69 ± 12.09	60.00 ± 0.00	<.001
Mean progression in diameter per second [mm/s]	0.39 ± 0.10	0.18 ± 0.03	<.001	0.44 ± 0.22	.19 ± .02	.025
Mean progression in depth per second [mm/s]	0.32 ± .09	0.13 ± 0.05	<.001	0.36 ± 0.24	0.11 ± 0.02	.035

Abbreviations: GI, generator impedance; LI, local impedance.

**FIGURE 10** Timing of occurrence of steam pops illustrated as Kaplan–Meier-analysis. Colors differentiate power levels. [Color figure can be viewed at wileyonlinelibrary.com]

LI correlates strongly with lesion diameter and depth in all power and ETC levels. LI drop and especially %LI-drop seem to be suitable parameters for assessing sufficient lesion formation in vivo. Therefore, additional monitoring of LI and changes in LI can increase the efficacy and safety of catheter ablation.

AUTHOR CONTRIBUTIONS

Andreas Wachter, Nico Erhard, Florian Englert, Hannah Krafft, Miruna Popa, Elena Risse: data collection, critical revision of article, approval of article. Marta Telishevska, Sarah Lengauer, Marc Kottmaier, Carsten Lennerz: statistics, critical revision of article, approval of article. Tilko

Reents, Gabriele Hessling, Isabel Deisenhofer, Felix Bourier: concept, statistics, critical revision of article, approval of article.

ACKNOWLEDGMENT

Open access funding enabled and organized by Projekt DEAL.

DATA AVAILABILITY STATEMENT

Research data are not shared.

ORCID

Fabian Bahlke MD  <https://orcid.org/0000-0002-6265-5403>

Carsten Lennerz MD  <https://orcid.org/0000-0002-1693-6474>

Felix Bourier MD  <https://orcid.org/0000-0003-4861-6595>

REFERENCES

- Nath S, DiMarco JP, Haines DE. Basic aspects of radiofrequency catheter ablation. *J Cardiovasc Electrophysiol.* 1994;5:863-876.
- Bourier F, Ramirez FD, Martin CA, et al. Impedance, power, and current in radiofrequency ablation: insights from technical, ex vivo, and clinical studies. *J Cardiovasc Electrophysiol.* 2020;31:2836-2845.
- Alken FA, Scherschel K, Kahle AK, Masjedi M, Meyer C. Combined contact force and local impedance dynamics during repeat atrial fibrillation catheter ablation. *Front Physiol.* 2022;13:1001719.
- Kautzner J, Neuzil P, Lambert H, et al. EFFICAS II: optimization of catheter contact force improves outcome of pulmonary vein isolation for paroxysmal atrial fibrillation. *Europace.* 2015;17:1229-1235.
- Mulder MJ, Kemme MJB, Allaart CP. Radiofrequency ablation to achieve durable pulmonary vein isolation. *EP Europace.* 2022;24:874-886.
- Bhaskaran A, Barry MA, Pouliopoulos J, et al. Circuit impedance could be a crucial factor influencing radiofrequency ablation efficacy and safety: a myocardial phantom study of the problem and its correction. *J Cardiovasc Electrophysiol.* 2016;27:351-357.
- Chinitz J, Michaud G, Stephenson K. Impedance-guided radiofrequency ablation: using impedance to improve ablation outcomes. *J Innov Card Rhythm Manag.* 2017;8:2868-2873.
- Das M, Loveday JJ, Wynn GJ, et al. Ablation index, a novel marker of ablation lesion quality: prediction of pulmonary vein reconnection at repeat electrophysiology study and regional differences in target values. *EP Europace.* 2016;19:775-783.
- Hussein A, Das M, Riva S, et al. Use of ablation index-guided ablation results in high rates of durable pulmonary vein isolation and freedom from arrhythmia in persistent atrial fibrillation patients. *Circ Arrhythm Electrophysiol.* 2018;11:e006576.
- Taghji P, El Haddad M, Philips T, et al. Evaluation of a strategy aiming to enclose the pulmonary veins with contiguous and optimized radiofrequency lesions in paroxysmal atrial fibrillation. *JACC Clin Electrophysiol.* 2018;4:99-108.
- Kanamori N, Kato T, Sakagami S, et al. Optimal lesion size index to prevent conduction gap during pulmonary vein isolation. *J Cardiovasc Electrophysiol.* 2018;29:1616-1623.
- Mattia LD. Prospective evaluation of lesion index-guided pulmonary vein isolation technique in patients with paroxysmal atrial fibrillation: 1-year follow-up. *J Atr Fibrillation.* 2018;10:1858.
- Chu GS, Calvert P, Futyma P, Ding WY, Snowdon R, Gupta D. Local impedance for the optimization of radiofrequency lesion delivery: a review of bench and clinical data. *J Cardiovasc Electrophysiol.* 2021;33(3):389-400.
- Bourier F, Popa M, Kottmaier M, et al. RF electrode-tissue coverage significantly influences steam pop incidence and lesion size. *J Cardiovasc Electrophysiol.* 2021;32:1594-1599.
- Nakagawa H, Wittkamp FHM, Yamanashi WS, et al. Inverse relationship between electrode size and lesion size during radiofrequency ablation with active electrode cooling. *Circulation.* 1998;98:458-465.
- Shapira-Daniels A, Barkagan M, Rottmann M, et al. Modulating the baseline impedance. *Circ Arrhythm Electrophysiol.* 2019;12:e007336.
- Matsuura G, Fukaya H, Ogawa E, et al. Catheter contact angle influences local impedance drop during radiofrequency catheter ablation: insight from a porcine experimental study with 2 different LI-sensing catheters. *J Cardiovasc Electrophysiol.* 2022;33:389-400.
- Martin CA, Martin R, Gajendragadkar PR, et al. First clinical use of novel ablation catheter incorporating local impedance data. *J Cardiovasc Electrophysiol.* 2018;29:1197-1206.
- Tsutsui K, Kawano D, Mori H, et al. Characteristics and optimal ablation settings of a novel, contact-force sensing and local impedance-enabled catheter in an ex vivo perfused swine ventricle model. *J Cardiovasc Electrophysiol.* 2021;32:3187-3194.
- Iwakawa H, Takigawa M, Goya M, et al. Clinical implications of local impedance measurement using the IntellaNav MiFi OI ablation catheter: an ex vivo study. *J Interv Card Electrophysiol.* 2021;63:185-195.
- Kumar S, Haqqani HM, Chan M, et al. Predictive value of impedance changes for real-time contact force measurements during catheter ablation of atrial arrhythmias in humans. *Heart Rhythm.* 2013;10:962-969.
- Tsutsui K, Kawano D, Mori H, et al. Characteristics and optimal ablation settings of a novel, contact-force sensing and local impedance-enabled catheter in an ex vivo perfused swine ventricle model. *J Cardiovasc Electrophysiol.* 2021;32:3187-3194.
- Shah DC, Lambert H, Nakagawa H, Langenkamp A, Aebly N, Leo G. Area under the real-time contact force curve (force-time integral) predicts radiofrequency lesion size in an in vitro contractile model. *J Cardiovasc Electrophysiol.* 2010;21:1038-1043.
- Takigawa M, Goya M, Iwakawa H, et al. Impact of a formula combining local impedance and conventional parameters on lesion size prediction. *J Interv Card Electrophysiol.* 2021;63:389-398.
- Lacko CS, Chen Q, Mendoza V, et al. Development of a clinically relevant ex vivo model of cardiac ablation for testing of ablation catheters. *J Cardiovasc Electrophysiol.* 2023;34:682-692.

How to cite this article: Bahlke F, Wachter A, Erhard N, et al. The influence of electrode-tissue-coverage on RF lesion formation and local impedance: Insights from an ex vivo model. *Pacing Clin Electrophysiol.* 2023;46:1170-1181. <https://doi.org/10.1111/pace.14807>